Using an Interferometric Synthetic Aperture Sonar to Inspect the Skagerrak World War II Chemical Munitions Dump Site

Torstein Olsmo Sæbø, Roy Edgar Hansen and Ole Jacob Lorentzen
Norwegian Defence Research Establishment (FFI)
Kjeller NO-2027, Norway
Email: torstein-olsmo.sabo@ffi.no

***Abstract*—In a collaboration between the Norwegian Defence Research Establishment (FFI) and the The Norwegian Coastal Administration, a HUGIN autonomous underwater vehicle (AUV) with a high resolution interferometric synthetic aperture sonar (SAS) was brought out to the Skagerrak World War II chemical munitions dump site. It mapped and documented parts of the site and located/relocated 35 shipwrecks. In this paper, we study the SAS technology for such applications. SAS technology have the potential to produce images and maps of very high resolution while maintaining large area coverage rates. There are, however, specific considerations to be taken when mapping and imaging shipwrecks which may be large complex elevated structures. We show data examples from the dump site, both of large shipwrecks and of small objects. We compare SAS images with sidescan images acquired earlier, and with multibeam echosounder data. We find SAS interferometry to be well suited for this type of documentation when operated and processed correctly.**

I. Introduction

Interferometric synthetic aperture sonar (SAS) technology can be used to obtain very high resolution in combination with long range in seabed imaging and mapping. The principle is based on combining recorded echoes using multiple pulses from different locations such that a larger (synthetic) array is constructed. This gives the potential to produce frequency and range independent along-track resolution [1]. Typical SAS systems have similar imaging geometry as sidescan sonars (SSS), providing large swath widths, but there are also significant differences between SSS and SAS [2], [3]. One strong benefit of SAS and SAS interferometry, is the potential to produce high resolution imagery while maintaining large area coverage rates [4]. Although being a fairly new technology, SAS operated from autonomous underwater vehicles (AUV) has become a major tool for documenting seabed conditions with various applications [5], [6], [7].

After World War II (WWII) around 168.000 tons of chemical munitions were loaded on 38 large ships and sunk in the Skagerrak Strait in the Norwegian trench, in the deepest waters between Norway and Denmark [8]. Some of the wrecks were torpedoed to sink. Other presumably broke into several parts before they hit the seafloor at around 600 m water depth (see Fig. 2). Most of the wrecks inside the dump site originate from the clean-up after WWII, but there are also some unknown wrecks in the area.

In a collaboration between the Norwegian Defence Research Establishment (FFI) and the The Norwegian Coastal Administration, a HUGIN autonomous underwater vehicle (AUV) with a dual frequency EdgeTech 2200 sidescan sonar where brought out to the dump site in 2009 [9], [10]. It mapped parts of the site and located 20 wrecks. In 2015, FFI went back with a HUGIN AUV equipped with a HISAS 1030 interferometric SAS [11] and re-visited the 20 wrecks and located 15 new ones. The survey of the site will be continued and finished in 2016. The Norwegian Coastal Administration will then use the sonar data along with core samples to evaluate the threat for chemical spill into the waters. Figure 1 shows the HUGIN AUV equipped with the interferometric SAS during launch from FFIs research vessel HU Sverdrup II.

Fig. 1. The HUGIN autonomous underwater vehicle with the HISAS 1030 interferometric SAS during launch from HU Sverdrup II.

In this paper, we consider SAS interferometry for imaging, mapping and documenting large shipwrecks. Wrecks may be elevated complex structures, imposing a worst-case for SAS, and we have compiled a set of considerations needed when performing a SAS survey of such targets. We also compare the sidescan imagery with the SAS imagery and present a brief and preliminary study of applying a EM 2040 multi-beam echo sounder (MBE) as a gap-filler for SAS.

978-0-933957-43-5 ©2015 MTS

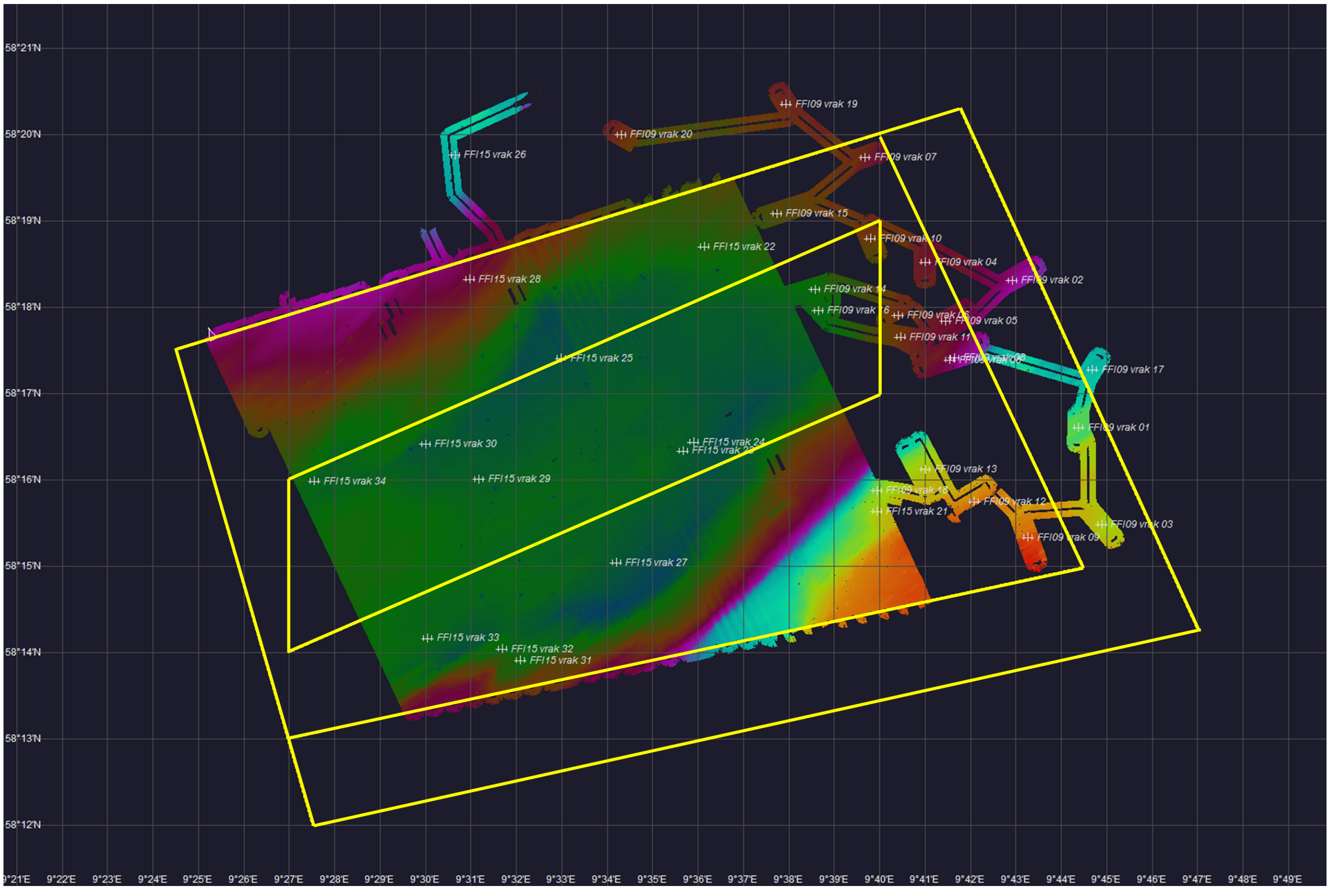

Fig. 2. Seafloor bathymetry of the dump site. The yellow boxes show the boundaries of the dump site defined in 1945 (smallest box), 1989 (medium box) and 2009 (largest box). The 35 wrecks we found in this years survey are also annotated. The depth range is from 532 m depth (red) to 717 m (blue)

II. Data acquisition and signal processing

In order to produce high quality SAS imagery and bathymetry there are two important stages: The acquisition stage and the signal processing stage. The first stage often gets too little attention, leaning on corrections in the signal processing. Post-mission corrections can only be achieved up to a certain point. For an AUV-survey on a reasonably flat seafloor, with weak currents and no large structures present (e.g. wrecks), a simple lawnmower pattern at any orientation at a fixed altitude will usually provide SAS rawdata of sufficient quality. Figure 3 shows an example of such a survey (although it turned out to be three wrecks present in the surveyed region).

On another mission we wanted to collect SAS rawdata past 20 known wrecks with as high quality as possible. The area was already surveyed in 2009 [10] so we did not need to get full coverage of the area. With known positions and orientations of each wreck these are some of the considerations in the acquisition stage:

- Track orientation: At broadside the entire wreck may be at an convenient range and shadows are less dominating. At end-fire there are less specular reflections.
- Range: At long range there is less layover [12] and less interferometric phase ambiguities [13], [14], while at short range the synthetic aperture is shorter, the SNR better and the shadows are shorter.
- Track linearity: Since a wreck is a complicated elevated structure, parts of it will have a significant focus plane error (i. e. offset from the true bathymetry). Thus, a non-linear track will cause defocus [15]. It is therefore better to strive a linear track than to run at fixed altitude. Crab should also be avoided.
- Coverage: Since an elevated structure always has shadows, multiple tracks are needed to get full coverage.
- Interference: As SAS is broadband, it is likely that other acoustic sources may interfere. Acoustic sources should be turned of when passing the wrecks.
- Global position accuracy: Both a recorded wreck position and the reported AUV position have uncertainties [16]. HiPaP acoustic positioning [17] or GPS-fixes may be important in order to limit this uncertainty.

Figure 4 shows the final mission plan. We managed two successful data acquisitions on each of the 20 wrecks. To reduce the position uncertainty we ran with HiPaP enabled.

In the second important stage, the signal processing stage, there are also a set of considerations:

- Image size: A large image may capture a large structure in one frame, but requires a linear track over a longer timespan.

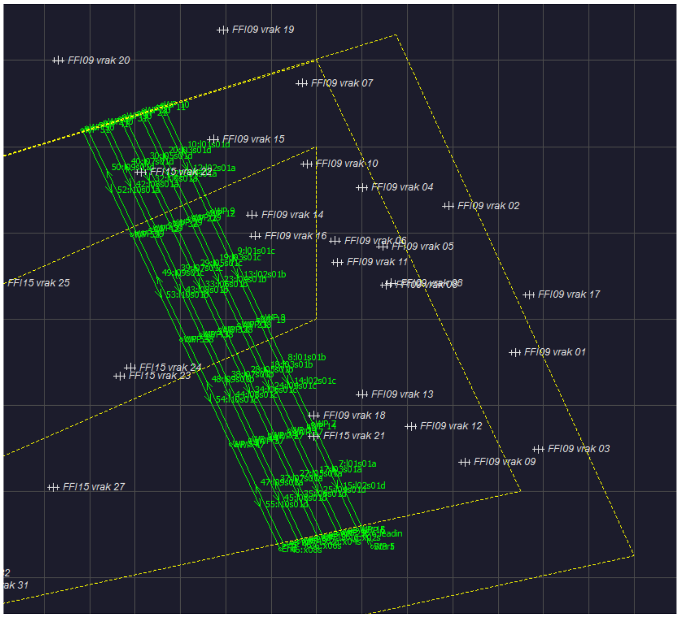

Fig. 3. Mission plan for April, 9th 2015, where we did not have a pre-survey.

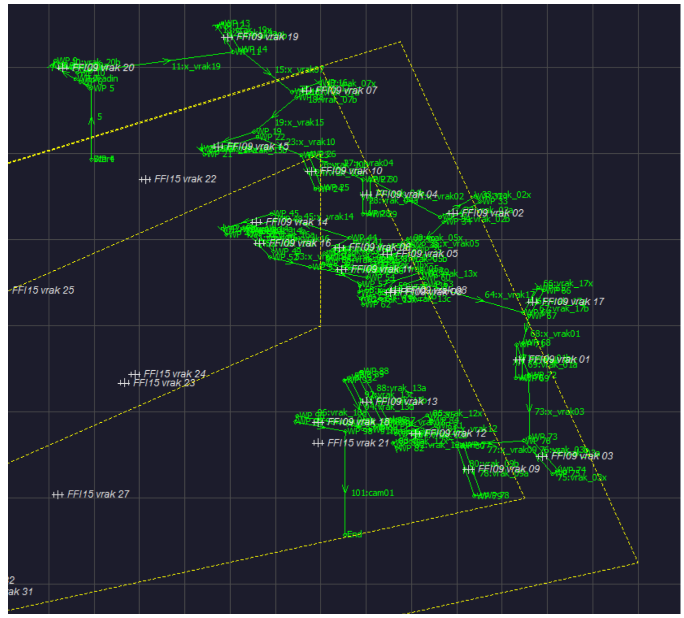

Fig. 4. Mission plan for April, 13th 2015, where we knew the locations of the 20 wrecks from the 2009 survey.

- Image resolution: Reducing the length of the SAS aperture may reduce defocus (but also reduce the along-track resolution).
- Image focus plane: A smooth plane will give an easier image to interpret, while a surface of higher degree can reduce defocus [15].
- Noise filtering: Noise may cause local damage to the estimated image and bathymetry, while noise filtering may cause local (time-filtering ping-data) or global (frequency-filtering SAS imagery) damage.
- Bathymetric resolution: Less resolution (larger estimation filter) results in less variance in the interferometric estimates [14], [18].
- phase estimation method: Standard phase differencing followed by 2π unwrapping may cause large regions of erroneous bathymetry [13], while a cross-correlation method may avoid this at the cost of some more random noise [19].

Figure 5 shows an example of how the choice of focus plane may affect SAS images. The left panel shows the image rendered on a smoothed version of the bathymetric estimate from sidescan data (best a-priori bathymetry) [20]. The right panel shows the image rendered on a sloping plane fitted to this surface. Clearly, the image in the left panel may be misleading as it seems like the hull is torpedoed.

III. Data visualization and interpretation

The sidelooking geometry makes SAS images (and sidescan images) of an elevated structure challenging to interpret. Layover, shadow, multiple scattering and transparency [14], [21] can all be dominating features. And quite frequently, schools of fish hoovering over the wrecks may further complicate the images. The upper panel of Fig. 6 shows an example SAS image of wreck 8. This is a 100 m long cargo vessel which has broken into two pieces. From the figure it is clear that a lot of seafloor information is lost due to shadows. It is also obvious that multiple scattering or transparency causes spurious echoes in the shadows which further complicate the interpretation (region A). Massive layover can be seen along the side of the left part of the ship (region B).

TABLE I. Typical HISAS 1030 system specifications.

Centre frequency	100 kHz
Wavelength	1.5 cm
Bandwidth	30 kHz
Frequency range	85-115 kHz
Along-track image resolution	3 cm
Cross-track image resolution	3 cm
Maximum range at 2 m/s	175 m
Area coverage rate	2 km^2/h
Interferometric baseline	28 cm
Interferometric baseline	18.7 wavelengths

Given the large amount of information contained in interferometric SAS data (image, bathymetry and interferometric coherence), the visualization can be a very important tool. The SAS image (i.e. the backscatter) has highest resolution and therefore provides most information about small objects and details. However, as we saw in Fig. 6, the sidelooking geometry complicates the interpretation of SAS images of elevated structures. The bathymetry is an complimentary source of information and can reveal information not easily deducible from the SAS image. The bathymetry has less resolution since it is generated from SAS images by using an estimation window of a certain size. The interferometric coherence is another important measure, since it is an estimate of the signal-to-noise ratio (SNR). Alone, it does not usually tell us much about the seafloor, but it is a reliable indicator of where we can trust the SAS image and the SAS bathymetry.

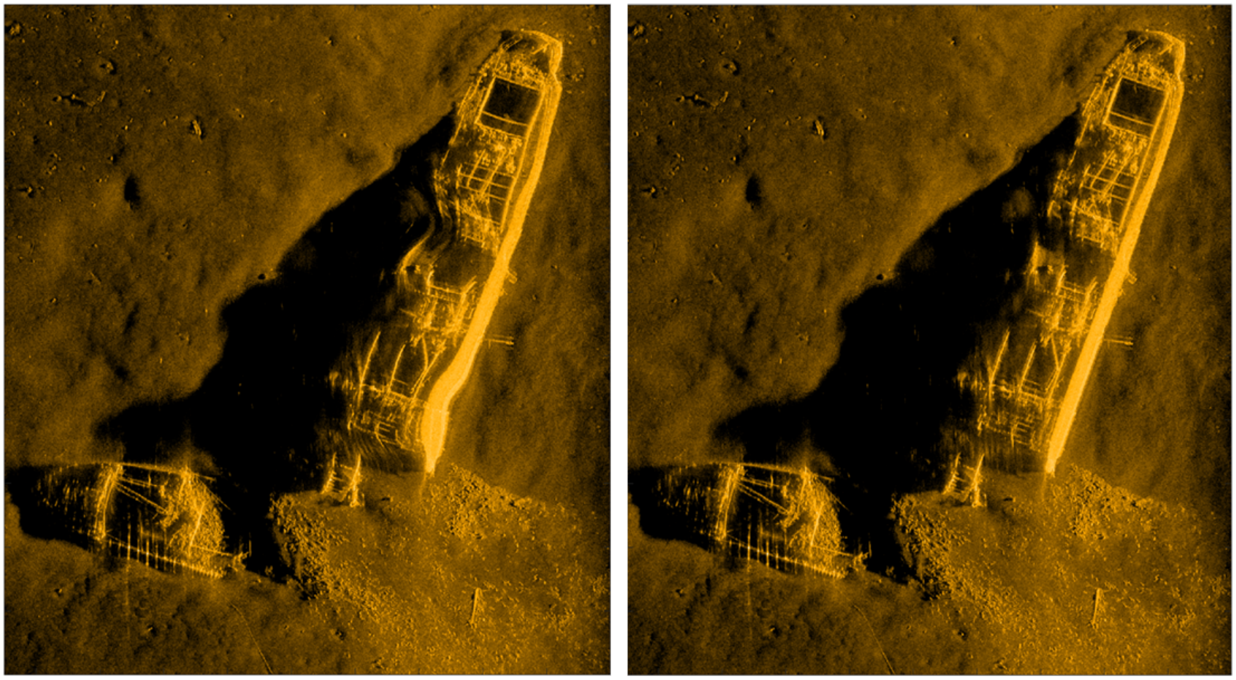

Fig. 5. SAS images of a cargo vessel (wreck 5) which has broken into two parts, along with debris from the wreck. Left panel: Image focused on the best a-priori bathymetry. Right panel: Image focused on a sloping plane fitted to the best a-priori bathymetry.

Table I shows typical specifications for the HISAS 1030 system. The SAS images are usually slightly oversampled into 2x2 cm grid. Complex cross-correlation filters of NxN pixels are then used to estimate the phase differences [19]. Default $N = 9$, which means that the distance between independent estimates in the bathymetry is 18 cm. However, we usually move the correlation filter pixel by pixel so that the gridding in the bathymetry also is 2x2 cm. We also store the estimated interferometric coherence in 2x2 cm.

In the upper panel of Fig. 6 there is clearly a lot of details in the SAS image, but to understand the 3D-shape of the wreck one has to rely on shadow-interpretation, which is a complicated and unreliable process. Instead we combine the image, bathymetry and interferometric coherence into a single plot. In the lower panel of Fig. 6 colour represents bathymetry, brightness the backscatter image, though the brightness is set to zero for coherence values below 0.66 (equivalent to 3 dB SNR). This visualisation technique is a powerful combination of detail and overview. From the colours it is easy to spot if the wreck is partially buried, if the seafloor is sloping or if the seafloor is disturbed by the wreckage. From the brightness, one can still make out details like individual shells of chemical munition or small structures on the wreck.

Another visualisation technique is synthetic movies, i.e. to put together a a set of 3D-renders from a different view angles into an AVI-file. In a single 3D snapshot it can be difficult to separate an object from the background (see Fig. 7), but the human mind is very good at combining images from a moving camera.

IV. Extracting information from the SAS images

The most compelling difference between the AUV survey in 2009 [10] and the one in 2015 is the introduction of a synthetic aperture sonar. For the 2009 survey, the primary sensor was a EdgeTech 2200 dual frequency sidescan, with one frequency band at 120 kHz and one at 410 kHz [22]. This is a powerful combination, since the lower band provides large coverage (comparable to the SAS coverage), while the higher band provides high resolution. However, this sonar can not provide large coverage and high resolution simultaneously. Neither can it achieve as high resolution as the SAS that has an *actual* along-track resolution of around 3 cm. For a 410 kHz sidescan to have 3 cm *theoretical* along-track resolution at 50 m range the array would have to be 6 m long. This is not achievable on most AUVs.

Figure 8 shows a SAS image of wreck 8 compared to a sidescan image from 2009 using the sidescan at 120 kHz. The range in the sidescan image is from 100-240 m, while the range in the SAS image is from 20-130 m so the comparison is not completely unbiased. However, while it can be difficult to identify the left part of the wreck as an actual wreck in the sidescan image, the SAS image shows a large amount of details which enables us to access the condition of the wreck and also possibly identify it.

In Fig. 9 we compare SAS imagery of wreck 18 with the sidescan at 410 kHz. At this frequency, the sidescan imagery contains a lot of details, due to its high resolution. However, the range is quite limited and the SAS image still superior in resolution. This can best be seen by comparing the debris scattered on the surrounding seafloor. In the sidescan image objects of around a meter is too blurred to identify, while in the SAS image it is possible to distinguish rocks of this size from man-made objects. As an example of how the SAS can be used for inspection of a chemical munitions dump site we have selected six image snippets from the SAS image in Fig. 8. Region A, B and C (seen in the upper panels of

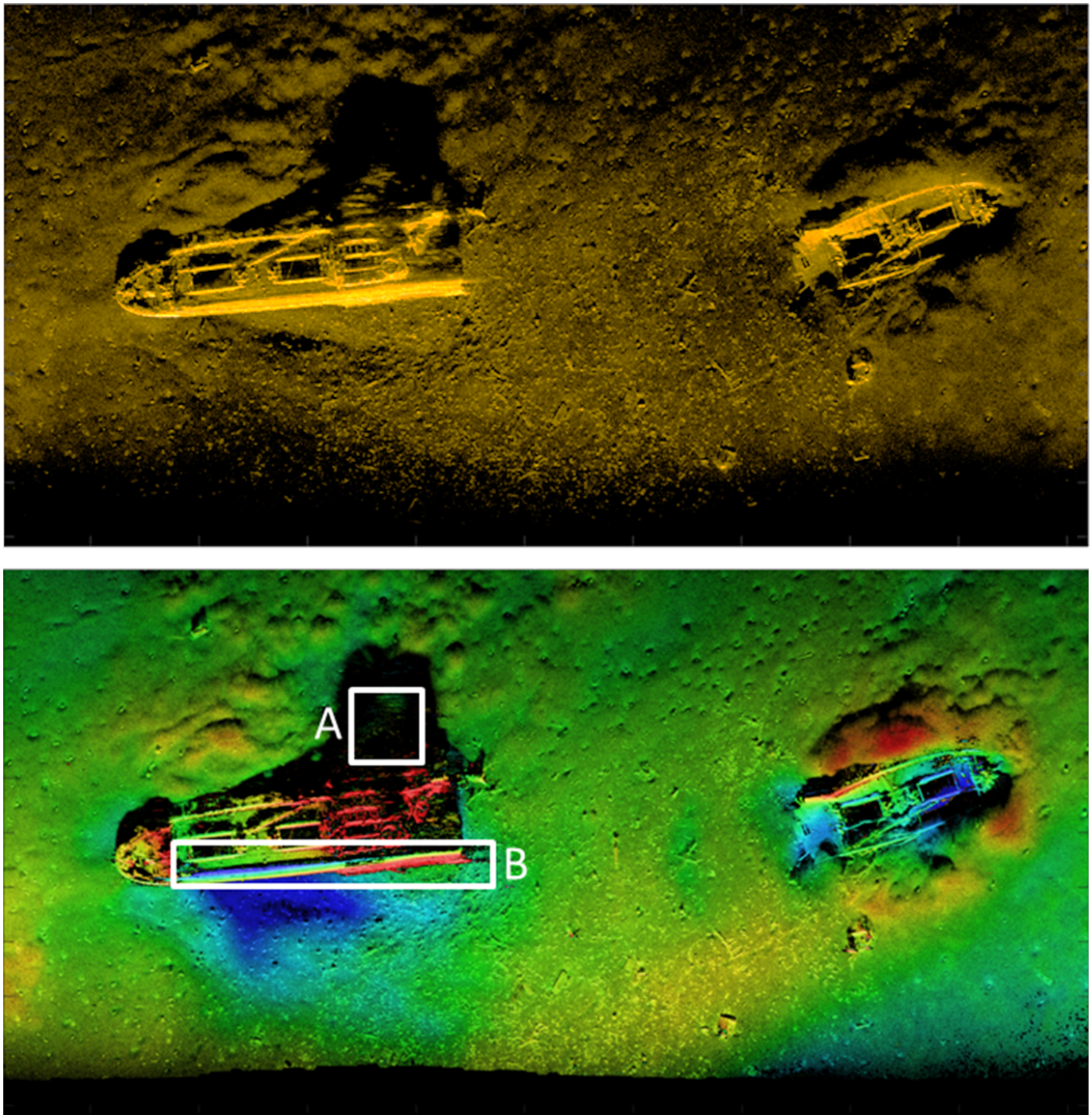

Fig. 6. Upper panel: SAS image of a 100 m long cargo vessel (wreck 8) which has broken into two parts, along with debris from the wreck The image is 200x100 m with 60 dB dynamic range. Lower panel: Combination of SAS image, bathymetry and interferometric coherence into a colour coded fusion. The depth range is from 642 m depth (red) to 646.5 m (blue).

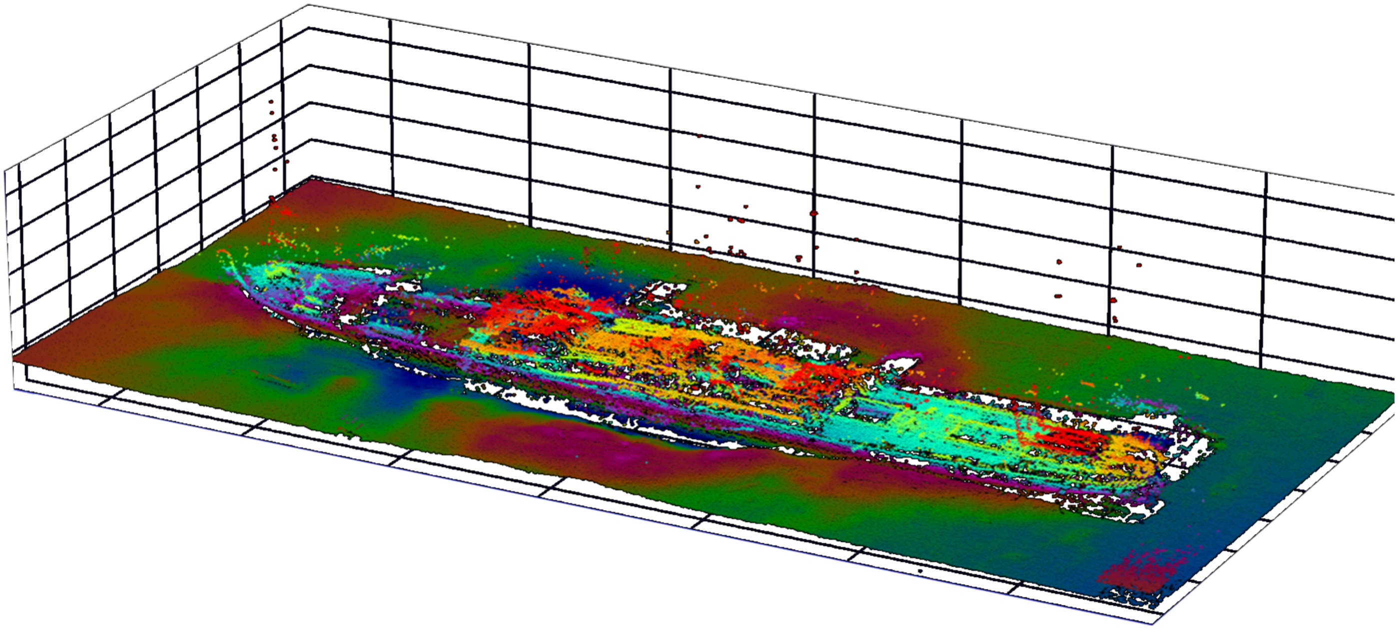

Fig. 7. Example 3D scatter plot of a 120 m long vessel (wreck 10), where all valid interferometric estimates (estimates with coherence above 0.66) are displayed as independent points. The depth varies from 660 m (red) to 668 m (blue).

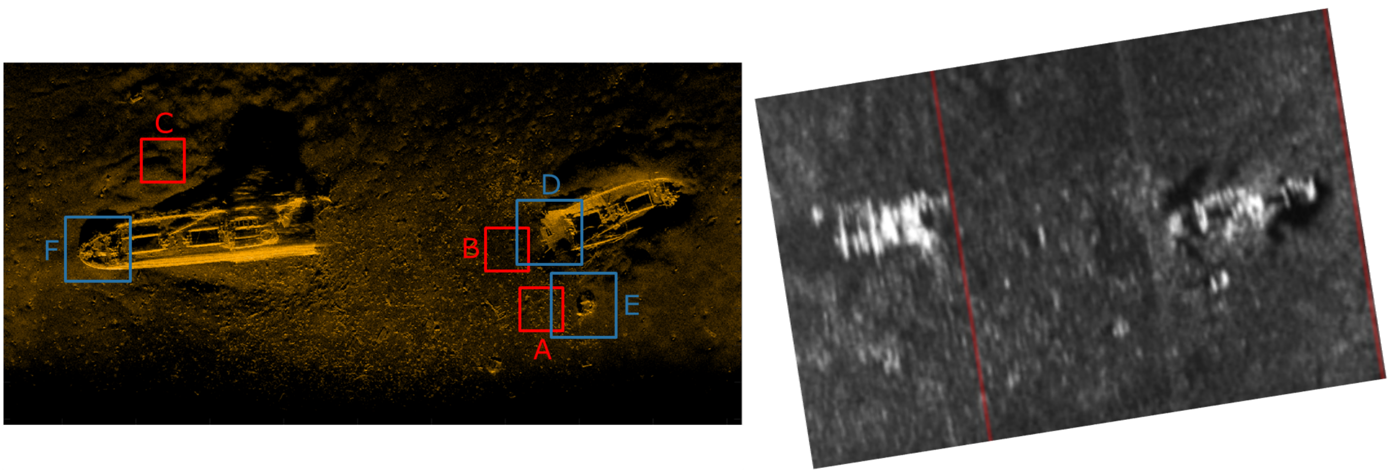

Fig. 8. Comparison of a 2015 SAS image of wreck 8 (left) and a 2009 sidescan image at 120 kHz (right).

Fig. 10) are all 10x10 m snippets with munition shells. It is possible to count each individual shell and classify each region into high density (0.5 shells/m^2), medium density (0.3 shells/m^2) and low density (<0.01 shells/m^2) regions. Without a high-resolution SAS image the classification would have to be performed using a remotely operated vehicle (ROV), which would have been extremely time consuming.

In the lower panels of Fig. 10 we show three 15x15 m snippets of the wreck (region D, E and F in Fig. 8). The left snippet shows the forward breach of the wreck which may tell us whether the wreck was used as target practice or if it broke in two during the dive to the seafloor. The centre panel shows debris from the wreck. Together with the detailed image of the aft section, such images can be used to give an initial assessment of the condition of the wreck. Off course, a full inspection of the degree of decomposition can only be achieved by optical camera combined with core samples. However, the SAS images gives a very good indication and can also be used as a basis for future surveys where changes in the SAS imagery can indicate decomposition of the wrecks.

V. Combining Interferometric SAS with a Multi-beam Echo Sounder

In addition to the HISAS 1030, the HUGIN HUS AUV is equipped with a EM 2040 multi-beam echo sounder (MBE) [23]. This MBE has better than one degree angular resolution which means that at ten meters range, the MBE has comparable bathymetric resolution to the SAS [24]. An MBE has also a favourable observation geometry compared to a sidelooking sonar when it comes to mapping of elevated structures. Shadow, layover and multiple scattering all disappear when the observation angle is vertical. However, a MBE observes out to 60 degrees from the vertical, which means that at the edges of the EM coverage these effects start to appear. Figure 11 shows

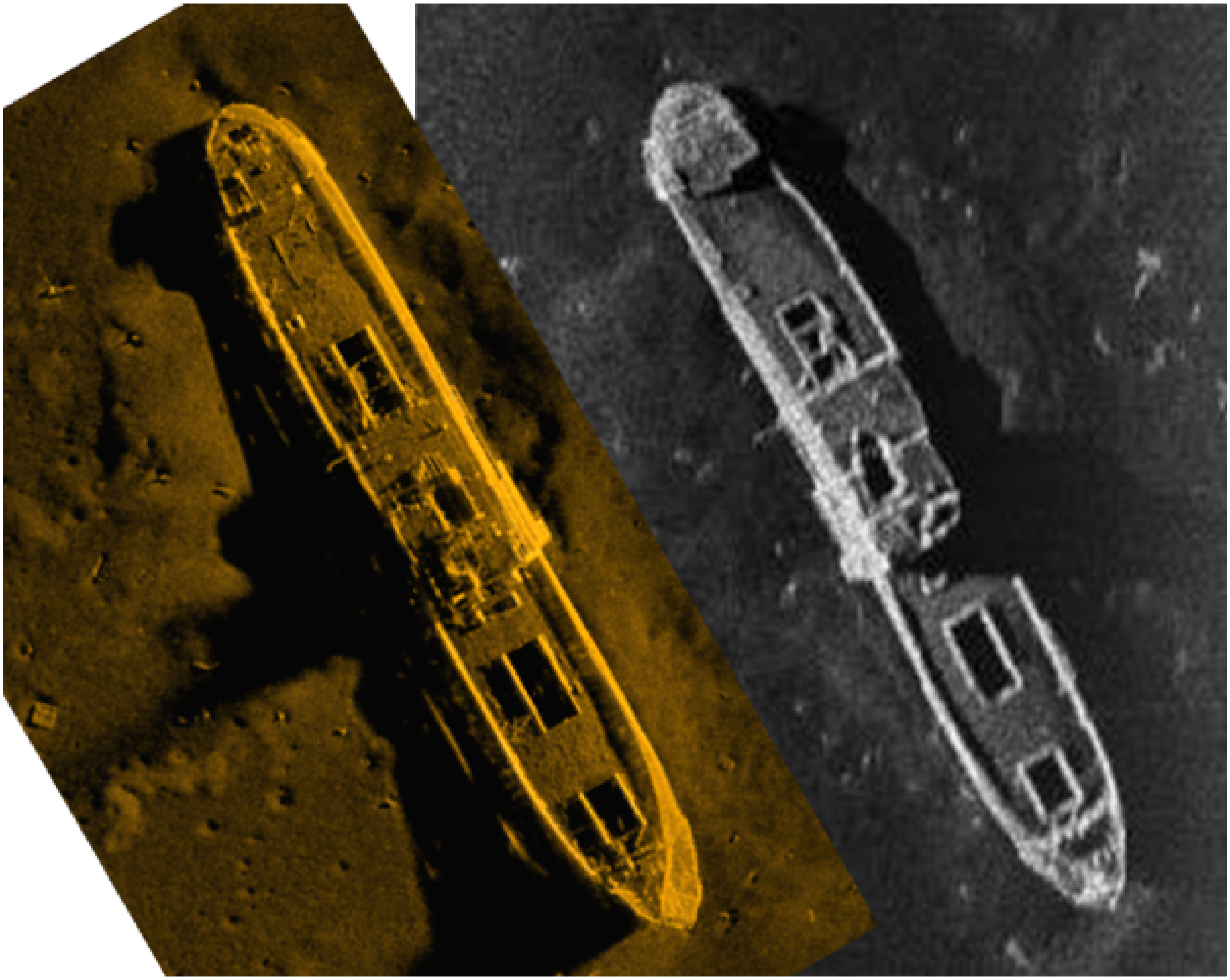

Fig. 9. Comparison of a 2015 SAS image of wreck 18 (left) and a 2009 sidescan image at 410 kHz (right).

a comparison between bathymetry from SAS interferometry and from the EM 2040. The data are from the same track, but is visualised in different software. Notice that the coverage is suboptimal for both sensors. The EM does not have full coverage, while the SAS has too steep incident angle (less than 45 degrees from the vertical) for parts of the wreck. Nevertheless a few observations can be made: There is a higher degree of detail in the SAS bathymetry - partly because this plot is a fusion of imagery, bathymetry and interferometric coherence. While the bathymetric resolution is comparable between the two sensors, the SAS image resolution is much higher. Another observation is that the SAS fusion image might be more complicated to interpret, due to the sidelooking geometry.

While a comparison between SAS and MBE is interesting, it is important to remember that they are *supplementary* sensors. This means that one should not use one of them, but combine them together. Figure 12 illustrates how the MBE can be used as a gap-filler for SAS in a bathymetric survey [25]. For a survey where the bathymetry is the desired output, a gap-filler can increase the area coverage up to 40% relative to using only SAS [25]. However, one has to remember that the MBE backscatter resolution is poorer than for SAS, so a fusion display of the data will have poorer resolution where the MBE is used as an imaging sensor.

VI. Summary

In this paper we have presented and discussed experimental data from two surveys of the Skagerrak World War II chemical munitions dump site. The site was first investigated using a HUGIN AUV equipped with an EdgeTech 2200 sidescan sonar in 2009 and again in 2015 using a HISAS 1030 interferometric SAS.

The HISAS 1030, a dual side interferometric sonar with 3x3 cm image resolution and around 18x18 cm bathymetric resolution, has proven to be a very powerful tool for wreck inspection. However, there are some special considerations needed when using SAS for imaging and bathymetric mapping of large structures. We have summarized these considerations

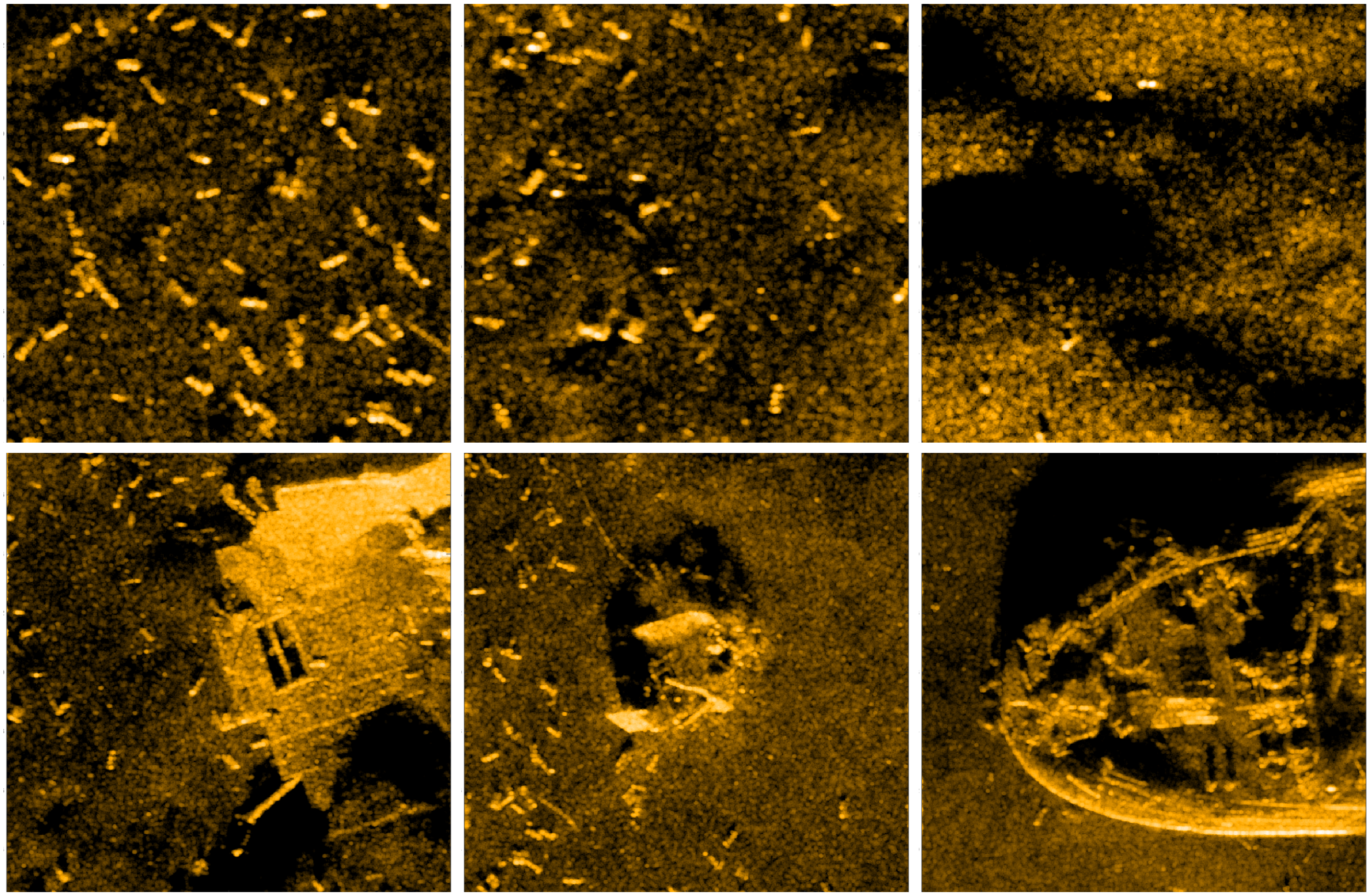

Fig. 10. Snippets from Fig. 8. The upper row shows 10x10 m snippets illustrating different densities of chemical munitions shells. From left to right: A (high density region), B (medium) and C (low). The lower row shows 15x15 m snippets from different parts of the wreck. From left to right: D (forward breach), E (debris) and F (aft section).

and categorised them into acquisition and processing stages.

We have compared the SAS data from 2015 with the sidescan data from 2009, and argued that the combination of resolution and area coverage rate is superior for the SAS system. We have also presented data which shows that 3x3 cm resolution is sufficient for an initial assessment of the condition of the wrecks along with classification of the surrounding debris.

Finally we presented data from the EM 2040 multi-beam echo sounder, and argued that this sensor can be used as a gap-filler for SAS in bathymetric surveys.

ACKNOWLEDGEMENT

The authors thank Stig A. V. Synnes and Petter Lågstad at the Norwegian Defence Research Establishment for valuable discussions. We would also like to thank The Norwegian Coastal Administration for letting us present the experimental data and the crew at HU Sverdrup II for contributing to the data collection.

REFERENCES

[1] R. E. Hansen, "Introduction to Synthetic Aperture Sonar," in *Sonar Systems*, N. Z. Kolev, Ed. Intech, September 2011, ch. 1, pp. 3–28. [Online]. Available: http://www.intechopen.com/books/show/title/sonar-systems

[2] X. Lurton, *An Introduction to Underwater Acoustics: Principles and Applications*, 2nd ed. Chichester, UK: Springer Praxis Publishing, 2010.

[3] P. E. Hagen, R. E. Hansen, and Ø. Midtgaard, "SAS and side scan sonar systems compared: Experimental results from HUGIN AUVs," in *Proceedings of Underwater Acoustic Measurements 2007*, Crete, Greece, June 2007.

[4] P. E. Hagen and R. E. Hansen, "Area coverage rate for Synthetic Aperture Sonars," in *Proceedings of Oceans '07 Europe*, Aberdeen, Scotland, June 2007.

[5] P. E. Hagen, T. Fossum, and R. E. Hansen, "Applications of AUVs with SAS," in *Proceedings of Oceans '08 Quebec*, Quebec, Canada, September 2008.

[6] A. R. Denny, T. O. Sæbø, R. E. Hansen, and R. B. Pedersen, "The use of synthetic aperture sonar to survey seafloor massive sulfide deposits," *Journal of Ocean Technology*, vol. 10, no. 1, pp. 48–65, 2015.

[7] Ø. Ødegård, M. Ludvigsen, and P. A. Lågstad, "Using synthetic aperture sonar in marine archaeological surveys - Some first experiences," in *Proceedings of Oceans 2013 MTS/IEEE*, Bergen, Norway, June 2013.

[8] T. Missianen and J.-P. Henriet, "Chemical munition dump sites in coastal environments," Federal Office for Scientific, Technical and Cultural Affairs (OSTC), Report, 2002.

[9] C. M. Hansen, P. E. Hagen, P. A. Lågstad, and J. A. Tørnes, "Case Study: Skagerrak Wrecks and Measures to Reduce the Environmental Risk," *Marine Technology Society Journal, The Legacy of Underwater Munitions Worldwide: Policy and the Science of Assessment, Impacts and Potential Responses*, vol. 43, no. 4, Fall 2009.

[10] P. A. Lågstad, "Kartlegging av vrak med HUGIN HUS i dumpefelt

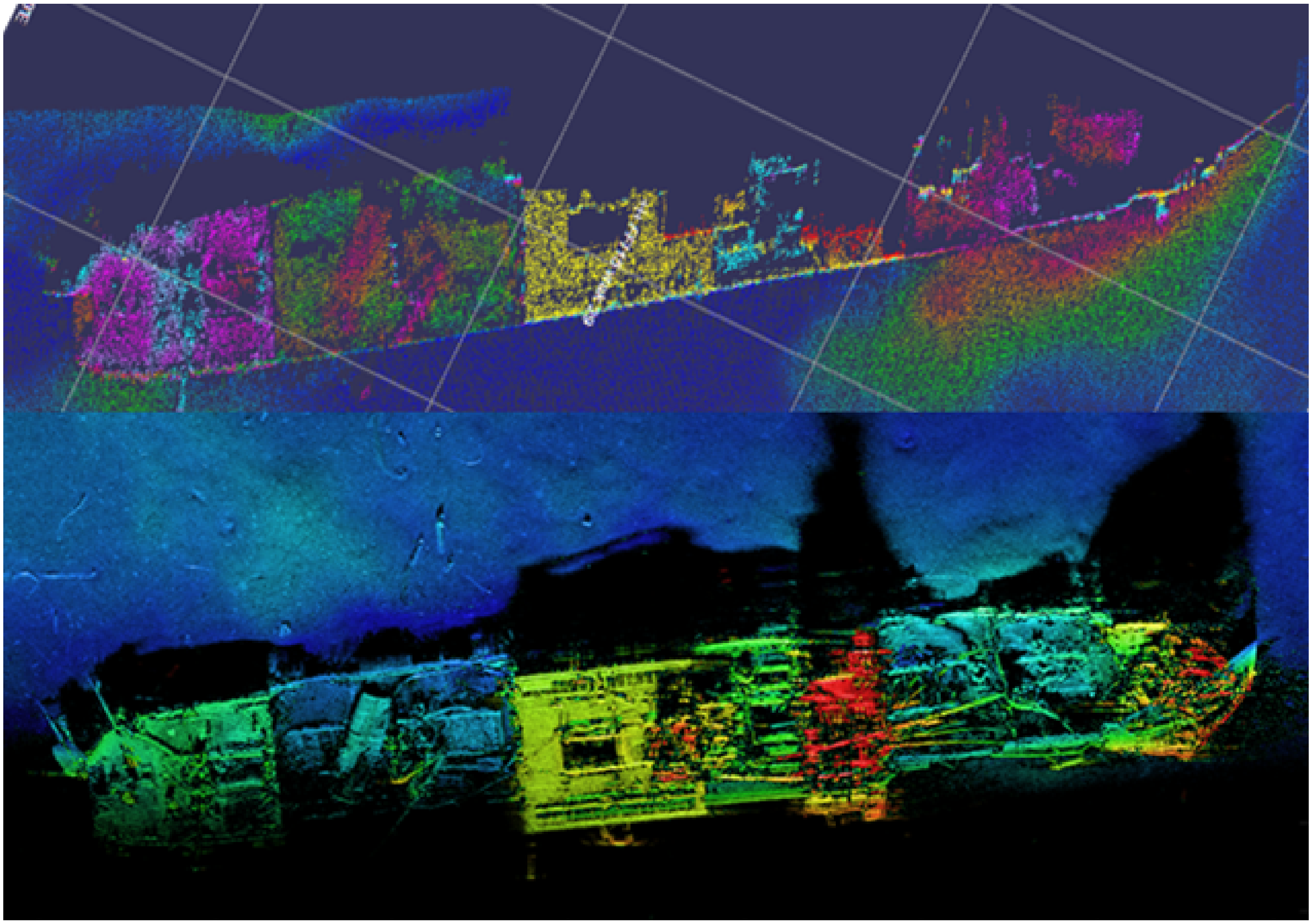

Fig. 11. Comparison of bathymetries of wreck 29 using the MBE (top) and the SAS (bottom). Both datasets are collected from the same track and the colour span is nine meters in both plots. The lower panel is a fusion of imagery, bathymetry and interferometric coherence. Note that the track is suboptimal for both sensors: The MBE does not have full coverage, while the SAS has too steep incident angle for parts of the wreck.

for kjemisk ammunisjon i Skagerrak," Norwegian Defence Research Establishment, FFI/RAPPORT (in Norwegian) 2009/02294, 2009.

[11] T. G. Fossum, T. O. Sæbø, B. Langli, H. J. Callow, and R. E. Hansen, "HISAS 1030 - high resolution interferometric synthetic aperture sonar," in *Proceedings of the Canadian Hydrographic Conference and National Surveyors Conference*, Victoria, BC, Canada, May 2008.

[12] G. Franceschetti and R. Lanari, *Synthetic aperture radar processing*. 2000 Corporate Blvd. Boca Raton, FL 33431, USA: CRC Press, 1999.

[13] D. C. Ghiglia and M. D. Pritt, *Two-dimensional phase unwrapping: Theory, algorithms, and software*. 605 Third Avenue, New York, NY 10158, USA: John Wiley & Sons, 1998.

[14] R. F. Hanssen, *Radar Interferometry: Data Interpretation and Error Analysis*. Dordrecht, The Netherlands: Kluwer Academic Publishers, 2001.

[15] R. E. Hansen, H. J. Callow, T. O. Sæbø, and S. A. V. Synnes, "Challenges in Seafloor Imaging and Mapping with Synthetic Aperture Sonar," *IEEE Trans. Geosci. Remote Sensing.*, vol. 49, no. 10, pp. 3677–3687, October 2011.

[16] B. Jalving, K. Gade, O. K. Hagen, and K. Vestgård, "A toolbox of aiding techniques for the HUGIN AUV integrated inertial navigation system," in *Proceedings of Oceans 2003 MTS/IEEE*, San Diego, CA, USA, September 2003.

[17] M. Mandt, K. Gade, and B. Jalving, "Integrating DGPS-USBL position measurements with inertial navigation in the HUGIN 3000 AUV," in *Proceedings of the 8th Saint Petersburg International Conference on Integrated Navigation Systems*, Saint Petersburg, Russia, May 2001.

[18] T. O. Sæbø, B. Langli, H. J. Callow, E. O. Hammerstad, and R. E. Hansen, "Bathymetric capabilities of the HISAS interferometric synthetic aperture sonar," in *Proceedings of OCEANS 2007 MTS/IEEE*, Vancouver, Canada, October 2007.

[19] T. O. Sæbø, S. A. V. Synnes, and R. E. Hansen, "Wideband interferometry in synthetic aperture sonar," *IEEE Trans. Geosci. Remote Sens.*, vol. 51, no. 8, pp. 4450–4459, August 2013.

[20] T. O. Sæbø, "Seafloor Depth Estimation by means of Interferometric Synthetic Aperture Sonar," Ph.D. dissertation, University of Tromsø, Norway, September 2010.

[21] J. C. V. Jakowatz, D. E. Wahl, P. H. Eichel, D. C. Ghiglia, and P. A. Thompson, *Spotlight-mode synthetic aperture radar: A signal processing approach*. P. O. Box 17, 3300 AA Dordrecht, The Netherlands: Kluwer Academic Publishers, 1996.

[22] "EdgeTech 2200 and 2205 AUV/ROV Sonars," http://www.edgetech.com/, 2015, [Online; accessed August, 20th 2015].

[23] *EM 2040, Multibeam echo sounder*, Rev. J ed., April 2015. [Online]. Available: www.km.kongsberg.com

[24] T. O. Sæbø and B. Langli, "Comparison of EM 3000 multibeam echo sounder and HISAS 1030 interferometric synthetic aperture sonar for seafloor mapping," in *Proceedings of the Tenth European Conference on Underwater Acoustics*, Istanbul, Turkey, July 2010, pp. 451–461.

[25] P. E. Hagen, "Gap filler sensors for SAS," in *Proceedings of Oceans 2011 MTS/IEEE*, Kona, HI, USA, September 2011.

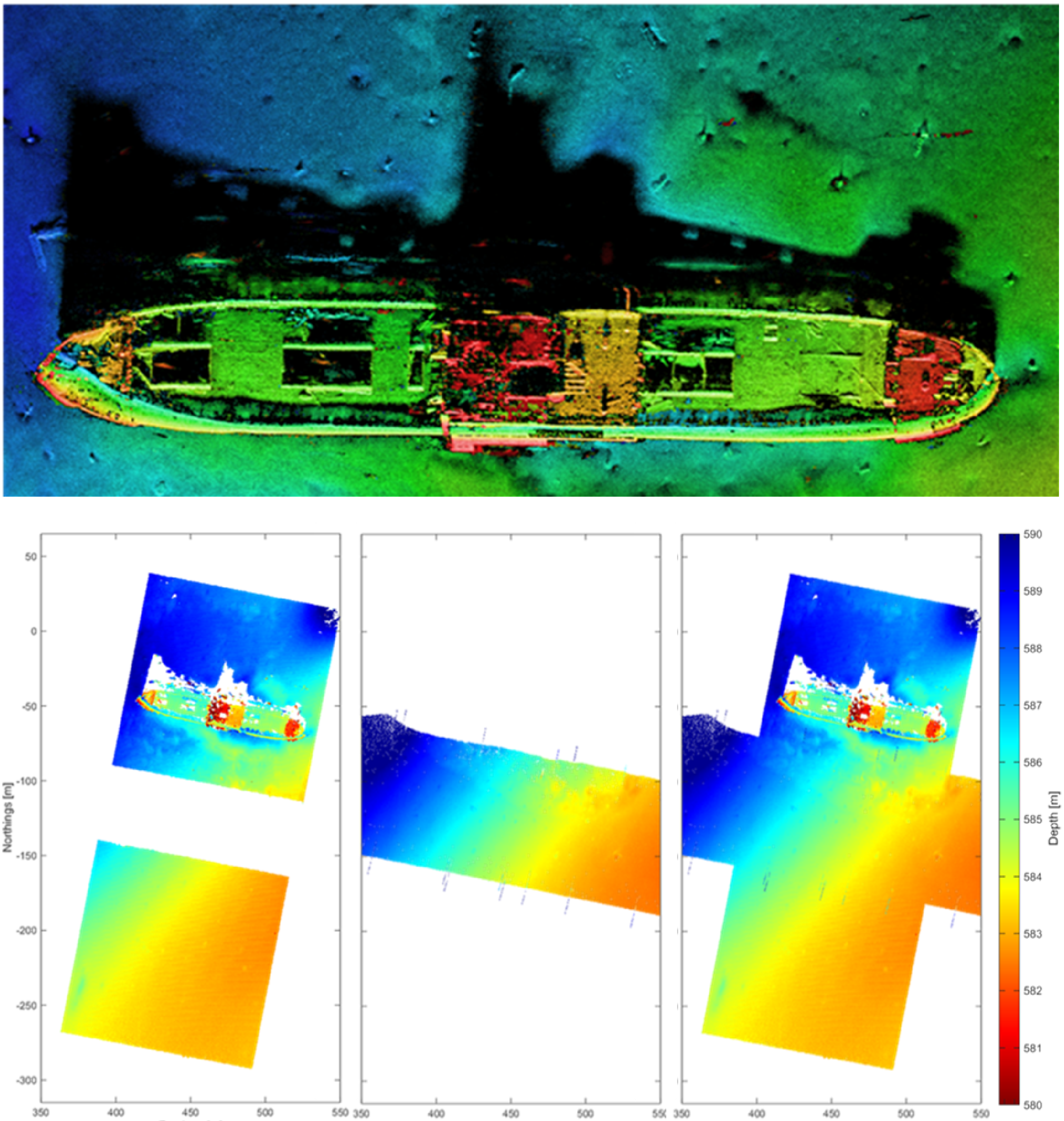

Fig. 12. Example fusion of SAS and MBE. The upper panel shows the SAS fusion image of wreck 18. The lower three panels show different bathymetries of the same wreck mosaicked into a 10x10 cm grid: SAS bathymetry (left), MBE bathymetry (centre) and fusion of SAS and MBE bathymetry (right).